Nanometal-Glass Hybrid Nanocomposites: Synthesis, Properties and Applications

Basudeb Karmakar*, Tirtha Som, Shiv Prakash Singh and Mithun Nath

Glass Science and Technology Section, Central Glass and Ceramic Research Institute (Council of Scientific & Industrial Research, CSIR, India), Kolkata 700032, India

In recent past research on nanometal-glass hybrid composites has been the centre of attraction across the globe particularly in the area of nanoscience and for the future nanotechnology. In this review, with a short historical background, its preparation by various multi-step techniques, properties and applications are briefly described. In addition, recently developed single-step in-situ thermochemical reduction methodology by these authors for synthesis of various nanometal-glass hybrid nanocomposites are described in details with their significant characteristic properties, relevant theories and applications. Here Au, Ag, and Bi metals are considered and the synthesized glasses are mostly based on antimony, bismuth and phosphorus oxides. Some of them are dichroic in nature, that is, they exhibit blue to green colourations in transmitted light and brown to reddish brown colourations in reflected light. The appropriate reasons for their dichroic character are still remained unsolved. Nanometal-antimony oxide glass nanocomposites have been found to enhance the photoluminescence upconversion intensities up to 11 fold when co-doped with rare-earth (RE) ions due to the plasmonic induced local field as enhanced by the effects of doped metal nanoparticles. The nanometal-glass hybrid nanocomposites, therefore, seem to be very promising for various nanophotonic applications (such as nanometal enhanced rare-earth luminescence, solar cell, light emitting diode, plasmonic integrated circuit, plasmon slot waveguide, etc.) that have presently emerged into a major field called '*plasmonics*'.

[Keywords: Nanometal, Glass, Nanocomposites, Single-step synthesis, SPR band, Plasmonics, Enhanced photoluminescence, Nanophotonics]

---

* Corresponding author, e-mail: basudebk@cgcri.res.in

Introduction

Metallic nanostructures are a subject of considerable interest in recent years because they are endowed with unique optical properties and functionalities contrast to their bulk counterparts.[1-11] In a bulk metal, the electrons are highly delocalized over large space i.e., least confined. This is because of the separation between the valence and conduction bands disappear, giving the metal its typical conducting properties. As we decrease the size of the metal and confine its electronic motion, the separation between the valence and the conduction bands becomes comparable to or larger than kT (about 200 cm^{-1}) and the metal behave like a semiconductor. This is shown in Fig. 1. Further confinement increases the energy separation and the material behave like an insulator. In the size domain at which the metal-to-insulator transition occurs, new properties are expected to arise which are possessed neither by the metal nor by the molecules or atoms forming the metal. Thus the properties of nanoparticles (NPs) gradually change from those of bulk material to molecular with decreasing particle size. In this intermediate range, metals with novel properties are quite noticeable.

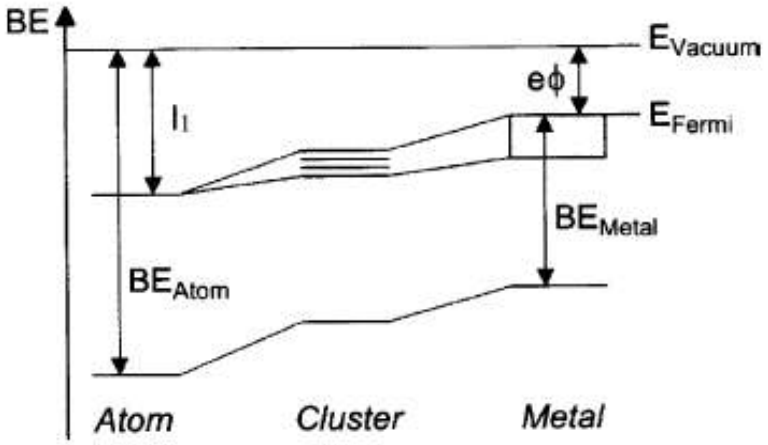

Fig. 1 - Evolution of electronic states from an atom via nanocluster to bulk metal (adapted from Ref. [3])

The coherent oscillation of the free electrons from one surface of the nanoparticle to the other is called the *'surface plasmon resonance'* (SPR). The optical science of metal nanoparticles and their potential application in photonics have very recently rapidly expanded into an important field called *'plasmonics'*.[4-6] One of the principle technologies that support modern optical communication, lasers, sensing and display systems is the photoluminescence of rare

earth ions (RE^{3+}), which involves the conversion of one type of energy (excitation light) into the photons of another energy (emission light). However, the small absorption cross-section of these RE ions has spawned numerous attempts to enhance the efficiency of these ions. Coupling RE^{3+} ions with metal nanoclusters have recently developed as an interesting alternative strategy to enhance the luminescence intensity of RE^{3+} ions and are likely to bring a renaissance in the field of solid state lasers. Besides absorption and scattering, SPR results in giant and highly localized electric fields around the metal NPs.[7-11] This conducting plasmonic metal nanostructures in the vicinity of RE ions are found to alter their free space spectral properties and greatly enhance the yield of their weak optical transitions by precise generation of intense electric fields, i.e., by local field enhancement (LFE) induced by SPR.[11, 12] This phenomenon is termed as *'nano metal enhanced fluorescence'* (NMEF). NMEF has not only emerged as a powerful tool in biotechnology[11-16] but it is also finding ever increasing applications in newly emerging nano-photonic technologies.[17] The induced high electromagnetic fields around the metal particles results in the enhancements of several optical processes like surface enhanced Raman scattering (SERS), surface enhanced fluorescence, non-linear optical processes, etc.[7-11]

However, for real application in nanophotonic devices, a major goal is to produce stable metal nanoclusters within suitable encapsulating hosts. It is well known that glasses possess several incredible properties like high transparency, ease of fabrication in desirable shapes and sizes, high durability and inertness, prevention of air oxidation of nanometals, low cost, ability of tailoring of properties, absence of high energy bond vibrations, etc. Besides these, they are most important from basic viewpoints. These have made glasses not only promising encapsulating hosts for lasing RE^{3+} ions but also for metal NPs. Consequently, nanometal- RE^{3+}-glass hybrid nanocomposites have created a center of enormous attention and many investigations are currently in progress.[18, 19]

Historical Background

Curiosity in the optical properties of colloidal metals in glass dates back to the *Roman Era* (753 BC to 476 AD). Although at that time there was no understanding of the underlying mechanisms which give rise to the spectacular colors of small metal particles but nanosized coinage metal (e.g., Au, Ag and Cu) particles were used as colorants in the stained glass windows of Cathedrals (red colored ruby glass), to color ceramics, enamel pottery, aesthetic

items, ornaments, etc. Sometimes they were also used to create complex optical effects such as dichroism. Perhaps the most famous example is the '*Lycurgus Cup'* that was manufactured around 400 AD.[20] The cup can still be seen in the British Museum and possesses the unique feature of changing color depending upon the light in which it is viewed. It is ruby red in transmitted light and green in reflected light. Analysis of the glass reveals that it contains a very small amount of tiny Au and Ag nanocrystals (~70 nm).[19, 20] Some landmark events in the history of nanometal-glass hybrid nanocomposites are listed in Table I.

In 1659, Johann Rudolf Glauber prepared colloidal gold as purple by reduction of gold salts by tin chloride in Germany. During 1679-1689, Johann Kunckel[21] used this purple gold for his glass works in Potsdam. In 1685, Andreas Cassius published the book *'De Auro'* incorporating the gold-based glass and enamel colours. After then it is known as *'Purple of Cassius'*. It was used in Meissen porcelain factory from and onward 1719. Around 1720, the *'Purple of Cassius'* reached China and was used in *'Famille Rose'* porcelain. The *'Purple of Cassius'* became, until today, the most popular enamel colour for pottery and porcelain. However, its chemical nature was a challenge for the scientists of the 19th century. In 1857, Michael Faraday prepared pure colloidal gold using phosphorous to reduce gold chloride. He recognized that the colour was due to the small size of the colloids. Around 1897, nearly 250 years after the discovery of the *'Purple of Cassius',* Richard Zsigmondy, a chemist working on gold at the Schott Glassworks in Jena, Germany showed that the *'Purple of Cassius'* consisted of colloidal gold and stannic acid. In recognition, he was awarded the Noble Prize in Chemistry in 1925. Various *'striking glasses'* were developed during 1924-1939 for generation of nanometals in glasses.[22]

However, the advent of modern characterization facilities like transmission electron microscopy (TEM was discovered in 1931) and scanning tunneling microscopy (STEM was discovered in 1938 but successfully re-developed for analysis of materials only in 1993) techniques, and introduction of quantum electrodynamics theories (Mie theory, Drude model, Maxwell Garnet Theory, Gans theory, etc) have directed research of metal-glass hybrid nanocomposites along with other branches of nanoscience and nanotechnology towards a new dimension[23,24]. Currently nanometal-glass hybrid nanocomposite is an interesting emerging area of research.[25-28]

Table I : Some landmark events in the history of nanometal-glass hybrid nanocomposites

Year (AD)	Event
Around 400	The '*Lycurgus Cup'* was fabricated with glass containing a very small amount of gold (Au) and silver (Ag) nanocrystals (~70 nm).
1659	J. R. Glauber prepared colloidal gold as purple by reduction of gold salts by tin chloride.
1679-1689	J. Kunckel used above purple for his glass works in Potsdam.
1685	Andreas Cassius published his famous book the *'De Auro'*. After this, the purple colour imparted by nanogold was known as '*Purple of Cassius'*. And purple colours of nanogold-based glasses, porcelains and enamels became very popular until today.
1719	'*Purple of Cassius'* was used in the Meissen porcelain factory.
Around 1720	'*Purple of Cassius'* reached China and there it was used in the *'Famille Rose'* brand porcelains.
1857	Michael Faraday prepared pure colloidal gold aqueous dispersions using phosphorous to reduce gold chloride in aqueous solutions. He recognized that the red colour was due to the small size of the colloids.
Around 1897	Approximately 250 years after the discovery of the '*Purple of Cassius'*, Richard Zsigmondy, a chemist working on gold colloids at the Schott Glassworks in Jena, Germany showed that the '*Purple of Cassius'* consisted of colloidal gold and stannic acid. In recognition for the answer of the long-waited unsolved problem, he was awarded the Noble Prize in Chemistry in 1925.
1908	Gustav Mie treated the optical properties of colloidal metals from the theoretical point of view and published his famous theory nowadays called the '*Mie theory'*.
1924-1939	Various *'striking glasses'* were developed for generation of different nanometals (e.g., gold, silver, etc.) in glasses.
1985-1989	Nanometals (e.g., silver) were used to enhance photoluminescence intensity of rare-earth ions in glasses and glass-ceramics. Perhaps, this may be the beginning of the journey of these nanocomposites towards modern nanophotonics.

Light Absorption by Metal Nanoparticles: Surface Plasmon Resonance

In noble metal nanoparticles, the decrease in size below the electron mean free path (the distance the electron travels between scattering collisions with the lattice centers) gives rise to intense absorption in the IR-visible-near-UV region. This result from the coherent oscillation of the free electrons from one surface of the particle to the other forming a electron cloud which is responsible for *'surface plasmon resonance'* (SPR).[6, 25, 26, 29, 30] More explicitly, under the influence of an oscillating electric field, the negatively charged conduction electrons perform a collective motion with respect to the positive-ion background, creating an effective charge at the surface that results in a restoring force[31]. For spherical particles this can be visualized as depicted in Fig. 2. The electron oscillation is therefore called a (localized) surface plasmon. Such strong absorption induces strong coupling of the nanoparticles to the electromagnetic radiation of light. This gives the metallic nanoparticles brilliant color. The surrounding dielectric medium exerts considerable influence on the position of the SPR band.[28] Upon excitation with incident radiation, the surface plasmons exist only at the interface of two media with dielectric constants of opposite sign. This condition is met in the IR-visible-UV wavelength region for dielectric/metal interfaces. Here dielectrics are air, water, glass, etc. Surface plasmons at the interface between a metal and a dielectric material have a combined electromagnetic wave and surface charge character, as shown in Fig. 3, in the generation of surface charge requires an electric field normal to the surface. This combined character also leads to the field component perpendicular to the surface being enhanced near the surface and decaying exponentially with distance away from it.

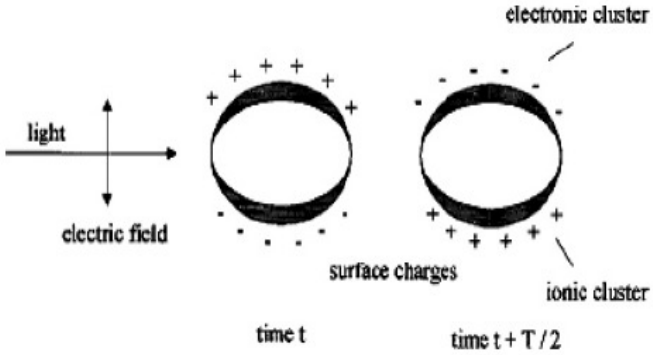

Fig. 2 - Schematic representation of creation of surface plasmon resonance (SPR) in spherical nanometal particles due to interaction of electromagnetic radiation. The induced dipole oscillates in phase with the electric field of the incoming light (adapted from Ref. 31)

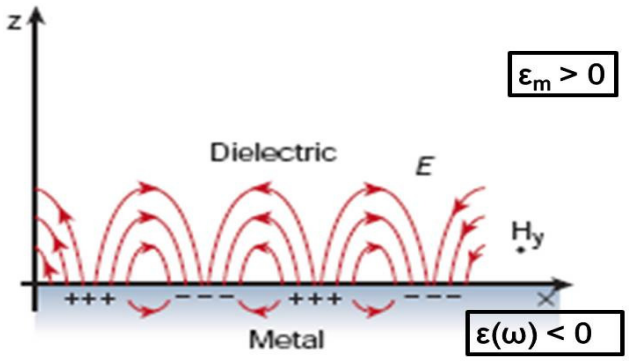

Fig. 3 - Surface plasmons at the interface between a metal and a dielectric material (adapted from Ref. 32)

Factors affecting Surface Plasmon Resonance

The frequency and intensity of the surface plasmon resonance (SPR) absorption bands are distinctive of the type of material (metal).[32] Metals only with free electrons (essentially the coinage metals Au, Ag and Cu, and the alkali metals) possess plasmon resonances in the visible spectrum, which give rise to such intense colors. For many metals like Pb, In, Hg, Sn and Cd the plasma frequency is in the UV; so no color effects are observed.[32] Since coinage metal (Au, Ag and Cu) nanoparticles and others like Bi can be easily detected by UV-Vis absorption and this is one of the reasons why they are more studied. These resonances are determined four factors: the density of electrons, the effective electron mass, and the shape and size of the charge distribution. In addition, the surrounding dielectric medium also exerts considerable influence on the position of the SPR band. Thus the optical effects in metallic nanostructures results from electrodynamics effects and from modifications of the dielectric environment.

Thus, the physical basis of light absorption by metallic nanoparticles or the intriguing optical properties of metal nanoparticles is due to localized SPR near the boundary between the metal nanostructures and the surrounding (dielectric) matrix. The surface plasmons exist only at the interface of two media with dielectric constants of opposite sign. This condition is met in the IR-visible wavelength region for air/metal, water/metal and glass/metal interfaces (where the frequency-dependent dielectric constant of a nano metal, $\varepsilon(\omega)$, is negative and that of air or water (medium), ε_m, is positive).[33]

The SPR bands are highly susceptible to the changes in sizes, spatial distribution and geometry of the nanostructures, particle density, inter-particle distance as well as the surrounding

environment.[34-36] Accordingly, the optical properties of metal nanoparticles can be controlled by adjusting these parameters. Generally, a red-shift of the absorption maxima is induced by increasing particle size, number density and increasing refractive index of the host matrix.[34-36] But in some cases, the blue-shifting (decrease in wavelength) of the SPR bands is also observed particularly for nanoparticles having diameter less than 20 nm.[35-38] This anomaly from the general behavior is due to electromagnetic field enhancement, called the dielectric confinement of the medium and quantum confinement (decrease in electron density) which is the direct consequence of the wave nature of the electrons. The shape of the plasmon band also changes with particle shape. In case of the small spherical particles a single plasmon band due to dipolar resonance is observed due to dipole plasmon resonance (sometimes denoted "dipole particle plasmon resonance" to distinguish from plasmon excitation that can occur in bulk metal or metal surfaces). But elongated nanoparticles may display two distinct plasmon bands related to transverse and longitudinal electron oscillations. Elongated particles may show two maxima if the aspect ratio is ≥ 4. The longitudinal resonance signal in case of gold, with an aspect ratio of 4, shifts from 520 to 770 nm.[39, 40] The longitudinal oscillation is very sensitive to the aspect ratio of the particles, so that slight deviations from spherical geometry can lead to impressive color changes.

The SPR peak of non-spherical metal NPs is generally red-shifted compared to spherical ones.[2, 5] As the size increases, the field across the particle become non-uniform, and this phase retardation broadens the dipole resonance and excites higher multipole resonances, such as the quadrupole, octupole, etc. leading to several peaks in the spectra.[40, 41] Higher modes of plasmon excitation can occur, such as the quadrupole mode where half of the electron cloud moves parallel to the applied field and half moves antiparallel. It is apparent that the dipole maximum rapidly shifts to longer wavelengths as the particle size increases beyond 70 nm (450 nm spectral maximum) revealing the quadrupole peak at about 420 nm. The observed spectral shift results from the *'spreading'* of the particle's surface charge over a larger surface area so that the surrounding medium better compensates the restoring force thus slowing the electron oscillations.[40, 41]

Several processes can damp the plasmon oscillations, such as electron scattering by lattice phonon modes, inelastic electron–electron interactions, scattering of the electrons at the particle surface, and excitation of bound electrons into the conduction band (interband

transitions).[40] Interband transitions can cause a substantially decreased efficiency of plasmon excitation, as is the case for Au and Cu, where there is significant overlap between the interband absorption edge and the plasmon resonance. For Ag, however, the absorption edge is in the UV (ca. 320 nm) and has little impact on the SPRs, which appear at wavelengths larger than 370 nm, accounting for the fact that excitation of the SPR in Ag particles is more efficient than for Au and Cu.[41] The bi-SPR peaks can also be generated due to the bi-modal distribution of metal nanoparticles.[42] Broadening of the SPR band is also observed for arbitrary shaped particles.[43]

Advantages of Glasses as Encapsulating Hosts

Although during the last two decades there has been an astounding progress in the wet-chemical synthesis of diverse metal particles of different shapes and sizes to understand their fundamental general properties, functionalities and modeling their optical responses[4, 7, 10, 44-47] but realization of the above emerging applications of plasmonic nanoparticles in active and real functional devices requires their synthesis/insertion within solid-state preferably transparent environment. Besides, metal nanoparticles must be embedded in solid dielectrics in order to avoid aggregation and the formation of the thermodynamically favored bulk material. Exploitation of glasses as encapsulating hosts for plasmonic metal nanoparticles (fabrication of metallo-dielectric nanocomposites) provides an opportunity to create a breed of nanoscale devices with attractive properties often due to the amalgamation of the properties of the glass host and the nano metal.

Glasses present some superior inherent advantages over other dielectrics. High transparency, mechanical strength, ease of fabrication in desirable shapes and sizes, ability to withstand high intensity radiation, preventing air oxidation of metal nanoparticles, etc. make glasses excellent encapsulating hosts for metal NPs for practical applications.[48-51] Glasses containing nanosized metal NPs are increasingly being appreciated for their potential application[48-53] as optical data recording disks and memory devices, optical waveguides, optical switches based on their nonlinear optical properties, photochromatic and color glass recycling industry, three-dimensional multicolored industrial art objects, etc. In all these applications the size, shape, number density, and distribution of the nanoparticles critically determine performance and properties of the nanocomposites.[48, 54-61] Such metal-glass nanocomposites also find other applications like solid-state lasers, sensors, dichroic polarizers, colored glasses,

ophthalmic lenses, display devices and optoelectronic materials due to nonlinear optical properties.[48-61] Since glasses are also promising hosts for encapsulating rare-earth (RE^{3+}) ions, consequently, an emerging application of metal-glass nanocomposites in the field of plasmonics is their development as substrates (hosts) capable of providing large electromagnetic enhancements or *'hot spots'* formation for nanometal-enhanced luminescence of RE^{3+} ions.

Multi-Step Synthesis of Nanometal-Glass Nanocomposites

Pioneering works on preparation of metal-glass nanocomposites and evaluation of their optical properties were performed by Doremus.[54, 55] Thereafter the metal-dielectric (glass) nanocomposites kept receiving significant exposures and are currently occupy a significant area of material science and nanotechnology.[48-53, 56-64] Preparation of nano metal doped conventional glass systems are not simple and demand multi-step techniques like sol-gel process, metal-dielectric co-sputtering deposition, direct metal-ion implantation, radio-frequency magneton sputtering, pulsed laser deposition, ion-exchange of thin plates followed by long time heat treatment at high temperatures in reducing (hydrogen) atmosphere or UV-light/X-ray/^{60}Co γ-radiation or high energy laser/synchrotron irradiation.[48-64]

However, the above customary techniques face some serious disadvantages. Firstly, only thin glass plates doped with metal nanoparticles can be obtained. Particularly the metal-dielectric co-sputtering deposition, direct metal-ion implantation and radio-frequency magneton sputtering methods are very costly. So, large-scale industrial production calls for simplified cost-effective techniques. Secondly, the sample may often get damaged on exposure to high intensity radiation. Thirdly, these methodologies are generally used to incorporate thin layers of spherical or quasi-spherical metal nanoclusters within high phonon (resonance vibration energy of the matrix) matrices like silicate, borate and phosphate glasses and the nanoparticle formation are only limited to the surface layers.[61] Fourthly, even on heat-treatment of the samples in hydrogen atmosphere for several hours at high temperature or laser irradiation for long duration there is hardly any shift of the SPR maxima.[62, 63] This is a severe disadvantage for many applications, like optical filters and surface enhanced fluorescence, where tuning of SPR band is essential.[7] Further it cannot be applied to low melting or low softening glasses. This is one of the reasons why mainly silicate and borate glasses have so far been used to fabricate metal-glass nanocomposites.

Moreover, it is known that the maximum local field enhancement occurs at mid-point between two interacting spherical metallic particles.[23-27] However, the field enhancement for a non-spherical nanoparticle is considerably greater than that of a spherical particle of comparable size.[23-27] Consequently fabrication of anisotropic or non-spherical nanoparticles (ellipsoids, rod-shaped, hexagons etc) with tunable optical properties is currently underway. So, development of simplified preparation techniques leading to the fabrication of new bulk dielectric (glass) matrices incorporating anisotropic metal nanoparticles in high yield with significant applications in the area of plasmonics is of paramount importance. Although anisotropic nanoparticles have been prepared in solutions[32-34] but they have hardly been prepared with solid matrices like glasses.

The evolution of SPR band of silver nanoclusters at 410 nm in optical absorption spectra of silver ion exchanged silicate glasses with heat-treatment temperature[62] is shown in Fig. 4. Figure 5 demonstrates the SPR band at 530 nm in the absorption spectra of glass containing gold nanoparticles induced by a femtosecond laser.[65] The development of SPR band of nano copper around 560 nm in alkali borosilicate glass[66] synthesized at 1150^0C in presence of C/CO oxygen buffer in shown in Fig. 6.

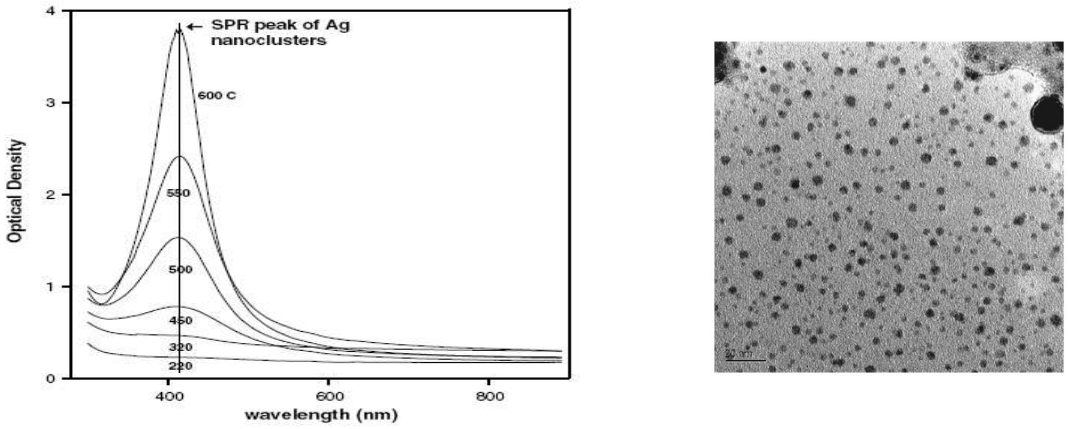

Fig. 4 – (a) Optical absorption spectra of silver nanoclusters embedded in silver ion exchanged soda glass matrix after annealing for 1 h at different temperature. (b) One of their TEM images (adapted from Ref. 62)

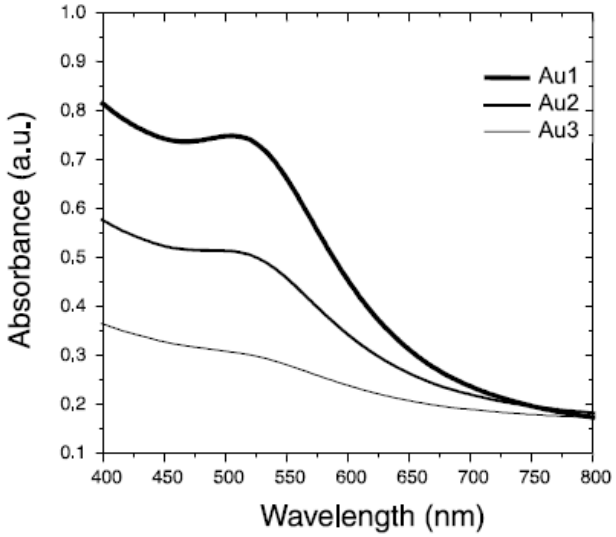

Fig. 5 - Absorption spectra of glass containing gold nanoparticles induced by a femtosecond laser (adapted from Ref. 65)

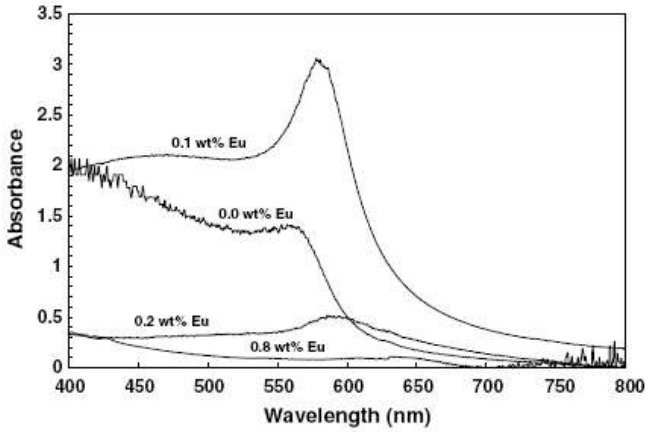

Fig. 6 - Absorption spectra of alkali borosilicate glass containing 0.25 wt.% Cu with different content of Eu synthesized at 1150^{0}C in presence of C/CO oxygen buffer (adapted from Ref. 66)

Single-Step Synthesis of Nanometal-Glass Nanocomposites

On contrary to the above traditional multi-step techniques, Karmakar and his coworkers [67-73] have very recently developed several simpler straightforward low-cost innovative single-step techniques involving fundamental glass chemistry to fabricate bulk metal-glass nanocomposites. Its flow-diagram is shown in Fig. 7. Several of these nanocomposites are

dichroic as well. This would be discussed in details in the next section. The techniques employed as well as the materials (glass based nanocomposites) can further be employed as suitable hosts for nanophotonics applications, particularly nano-metal enhanced fluorescence of rare-earth ions. In this review, we shall discuss each of these techniques along with their superiority and thermochemical mechanism. Besides, the effects of particle size, shape and concentration, refractive index of the dielectric (here glass) matrix, quantum and dielectric confinements on the surface plasmon resonance (SPR) bands of the mental nanoparticles have been considered and explained with relevant electrodynamics theories.

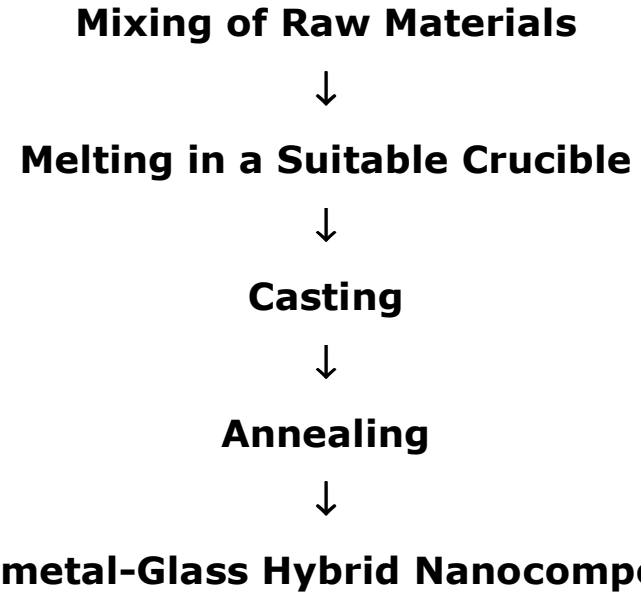

Fig. 7 - Flow-chart of single-step methodology for synthesis of nanometal-glass hybrid nanocomposites

Dichroic Nanometal-Glass Nanocomposites

The best example of dichroic nanometal-glass nanocomposites is the *'Lycurgus Cup'* which is green when illuminated from outside and red when illuminated from inside.[20]. It is made up of glass nanocomposites with about 70 nm sized gold and silver metal nanoparticles. This fact was mentioned earlier. The deep red color of gold-ruby red *'striking glasses'* on further heat-treatment starts to fade and changes into dichroic *'saphirin glasses'*. It produces weak blue

transmission colors and strong brown reflection colors. The blue and brown colors were attributed to small and large spherical gold colloidal particles respectively.[22]

Regarding the origin of dichroism, earlier researchers observed that the color of this well-renowned gold-ruby glass varies with heat treatment. It was assumed that small sized gold particles (3-5 nm) act as nuclei and they grow under proper conditions (heat treatment) through the deposition of gold atoms on their surfaces. At 700 °C, some of the gold crystals grow at the expense of smaller ones. At optimum sizes of 5–60 nm a strong ruby color is yielded. Particles which become considerably larger, 200-500 nm, contribute very little to the absorption. Their main function is scattering and reflection of light. Scattering occurs whenever a beam of light is passed through a transparent medium containing in suspension of small particles, the refractive index of which differs from that of the medium. Glasses containing particles of this range (Saphirin glass) give blue color in the transmitted and brown color in the reflected light and absorption wavelength shifts from 530 to 570 nm with successive crystal growth.[22] At that time visual examination by means of ultra-microscope did not reveal the actual shape of the particles.[22] Later on the advent of commercial transmission electron microscopy (TEM), which was discovered in 1931, made possible the determination of actual shapes of gold particles.[74] In 1940, by means of TEM, Borries and Kausche[22] confirmed the presence of anisodimentional Au crystals. Particles which are sufficiently large and which deviate in shape from sphere orient themselves parallel and produce birefringence. Recently, although Schreiber et al.[66] have proclaimed that $(Cu)_n^0$ nanoparticles of certain sizes (no information about shapes was given) formed by a combination of redox and nucleation processes give rise to dichroism but now it is also a well acknowledged fact that prolate ellipsoid Ag NPs having an aspect ratio around 1.2 exhibits the phenomenon of dichroism.[39, 62]

Production of dichroic glasses generally involves deformation of embedded spherical nanoparticles (in silicate based glasses) into ellipsoidal NPs by intense irradiation with ultrashort laser pulses[59] or stretching metal-doped glasses in their softening range.[58] In recent times, Hofmeister and his coworkers[58, 75] have produced silicate based dichroic glasses by deformation of embedded spherical nanoparticles into ellipsoidal nanoparticles by these techniques. Their elliptical morphologies were confirmed by the TEM analysis. Fort, et al[76] have also established that the dichroic character is caused by the elliptical shaped nanoparticles and arises due to difference in polarizations, that is, electron oscillations along the major (longitudinal) and minor

(transverse) axes of a polarizable ellipsoidal nanoparticles during interaction with electromagnetic waves.

The present authors[67-70, 72, 73] have carried out several studies in this view. It is understood that the dichroic character of nanogold-antimony oxide glass nanocomposites[67-69] caused by the elliptical nanogold particles (see Figs. 9 a-c). On other hand, the dichroic nanogold-tin phosphate glasses[73] contain spherical nanogold particles of wide size variation (see Figs. 9 d-f). In the case of nanosilver-bismuth oxide glass nanocomposites,[72] dichroism arises due to both hexagonal and spherical silver nanoparticles (see Figs. 9 g-i).

From these facts, it is clear that both spherical and non-spherical gold or silver nanoparticles could exhibit dichroism. It is very difficult to assign the dichroism exclusively either to the spherical or to the nonspherical shaped nanometallic particles. The appropriate reasons for their dichroic character are, therefore, remained unsettled. Therefore it needs further studies.

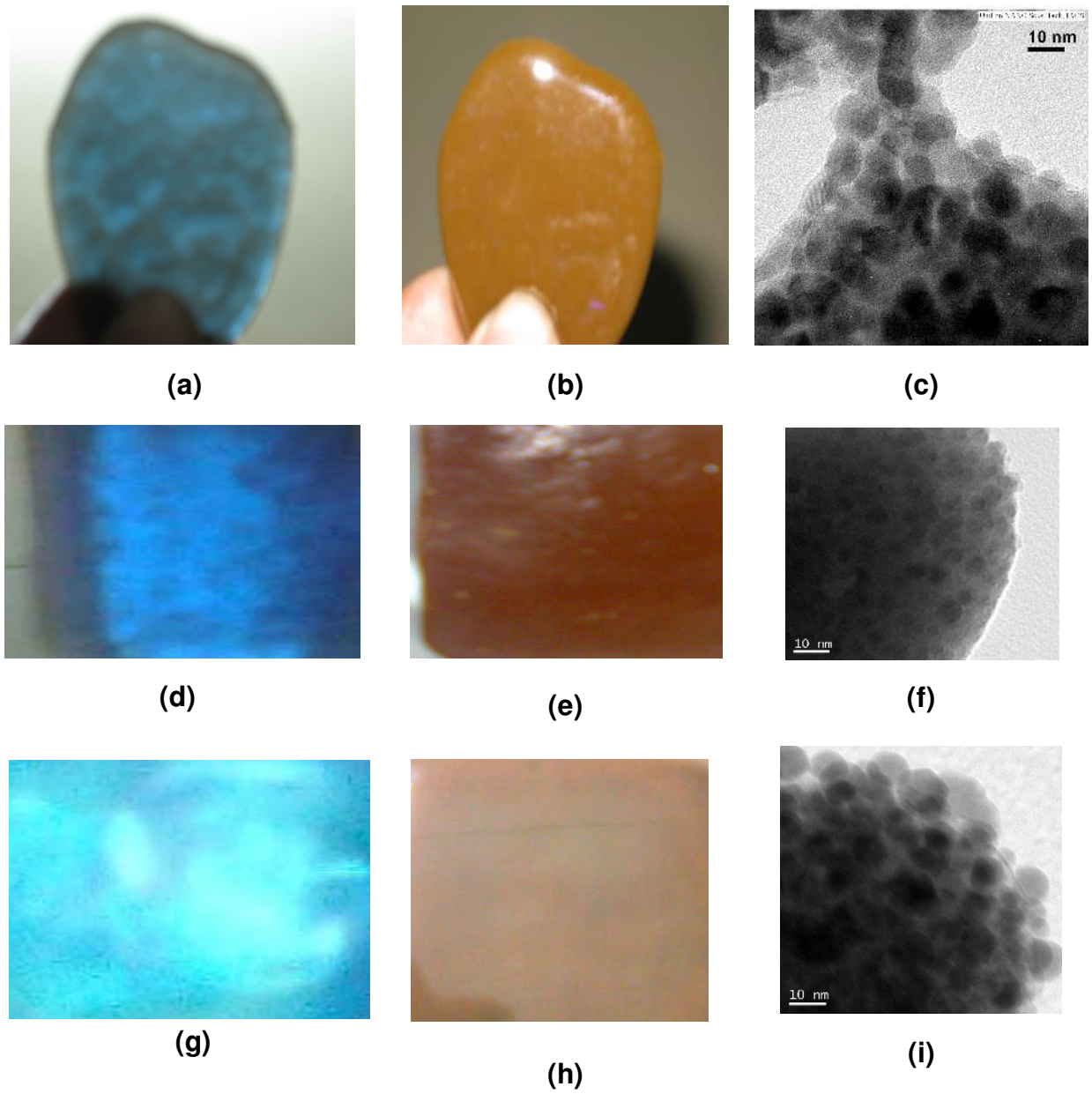

Fig. 8 - Nanogold-antimony oxide glass hybrid nanocomposite: (a) transmitted blue color, (b) reflected brown color, and (c) TEM image shows the elliptical shape of its nanogold particles (adapted from Ref. 67-69). Nanogold-tin phosphate glass hybrid nanocomposite: (d) transmitted deep blue color, (e) reflected reddish brown color, and (f) TEM image shows the spherical shape of its nanogold particles (adapted from Ref. 73). Nanosilver-bismuth oxide glass hybrid nanocomposite: (g) transmitted blue color, (h) reflected brown color, and (i) TEM image shows the combination of hexagonal and spherical shapes of its nanosilver particles (adapted from Ref. 72)

Nanometal-Antimony Glass Hybrid Nanocomposites: Synthesis, Effects of Particle Size, Composition and Refractive Index of Glass Host

Preparation of high antimony(III) oxide (Sb_2O_3) containing monolithic glasses encounter serious limitations. Available reports on synthesis of antimony glasses show that they are usually yielded as tiny pieces or pulverized form incompatible for practical applications in photonics. This is firstly because of the low field strength (0.73) of Sb^{3+} cation makes Sb_2O_3 a poor glass former. Secondly, the intense vaporization of Sb_2O_3 during melting and high devitrification during casting has made their synthesis extremely difficult Hence, the area of nano metal-embedded Sb_2O_3 based glasses and nanocomposites had remained totally unexploited because of their difficulties in preparation particularly in the bulk monolithic form.

Very recently, Som and Karmakar[67-70] exemplified for the first time a new single-step melt-quench thermochemical reduction technique for the fabrication of monometallic and bimetallic (Au-Ag) antimony oxide glass hybrid nanocomposites. The idea involved the employment of a suitable antimony oxide based glass matrix, K_2O-B_2O_3-Sb_2O_3 (KBS) and K_2O-B_2O_3-Sb_2O_3-ZnO (KBSZ), which itself has a reducing property mild enough to generate nano sized metallic particles. It must be mentioned here that oxides having very high reduction capabilities assists in the formation of larger particles. It is noteworthy that we are the first to report the synthesis and plasmonic properties of nanometal-antimony oxide glass nanocomposites.

It was observed that all Au-doped antimony oxide glasses were dichroic, i.e., they transmitted the blue color (see Fig. 8a) and reflected the brown to reddish-brown (see Fig. 8b) light. The intensity of the reflected brown color increases with increase in Au^0 concentration. The UV-Visible absorption spectrum is the most important tool to detect the formation of noble metal NPs and SPR bands. Typical UV-Vis-NIR absorption spectra of elliptical Au nanoparticles with increasing gold concentration and particle sizes in K_2O-B_2O_3-Sb_2O_3 (KBS) glasses are shown in Fig. 9. The absorption spectrum of the undoped glass (curve-a) shows absence of any features indicating the base glass matrix is transparent in the spectral region of interest to this study. The absorption spectra of the Au doped glasses (curves b-g) display well-defined broad plasmon (SPR) absorption bands (610-681 nm) characteristic of nano sized Au^0.

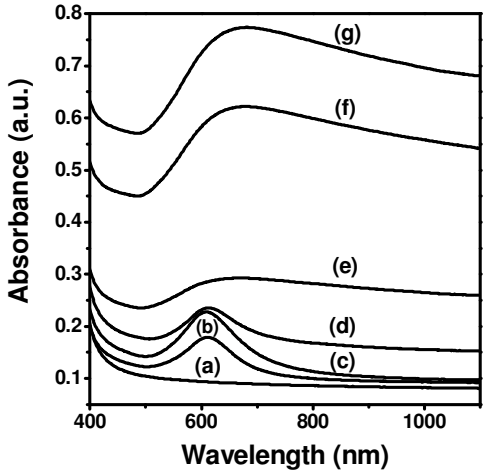

Fig. 9 - UV-Vis absorption spectra of (a) base glass and (b-g) with increasing nanoparticle concentration, size and decreasing inter-particle distance (a. u. represents absorbance unit) (adapted from Ref. 69)

Although a number of theoretical models and methods have been suggested, the original classical model by Gustav Mie[77] is often used to describe the shape of the plasmon absorption band of metal nanoparticles. According to the Mie theory, for a collection of small spherical non-interacting metallic spheres (low particle density) in the quasi-static regime of radius ($R << \lambda$) having a dielectric function (complex) that depend on the angular frequency of light ω, $\varepsilon_{Au}(\omega) = \varepsilon_1(\omega) + i\varepsilon_2(\omega)$, embedded in a medium of dielectric constant ε_m (real), and sizes much smaller than the wavelength of light about 25 nm for gold particles), only the dipole oscillations contribute significantly and the extinction (absorption + scattering) coefficient C_{ext} is given[5, 25, 38] by

$$C_{ext} = [18\pi N V_{np} \varepsilon_m^{3/2} / \lambda] \times [\varepsilon_2 / \{(\varepsilon_1 + 2\varepsilon_m)^2 + \varepsilon_2^2\}] \quad (1)$$

where N is the number of particles, V_{np} the volume of each particle in the quasi-static regime ($V_{np} = 4\pi R^3/3$). The real (ε_1) and imaginary (ε_2) parts of the dielectric function $\varepsilon_{Au}(\omega)$. If ε_2 is very small or weakly dependent on ω then, from Eq. (1), the absorption maximum corresponding to the resonance condition is produced when $\varepsilon_1 = -2\varepsilon_m$, leading to a disappearing denominator. Hence, a SPR absorption is produced at optical frequency ω at which the resonance condition $\varepsilon_1 = -2\varepsilon_m$ is fulfilled.[5, 25, 33, 34, 38]

According to Eq. (1), the SPR band is independent of size within the dipole approximation. But practically the plasmon band width increases with decrease in particle size for particles smaller than 20 nm. The size dependence arises from the size dependence of the dielectric constant $\varepsilon_{Au}(\omega, d)$ of the metal. This is referred as "intrinsic size effect".[5, 38] For nanoparticles of larger dimension (>25 nm for gold nanoparticles), significant contributions are made by higher-order (quadrupolar) charge cloud distortion of conduction electrons. These contributions induce drastic red-shift (from 610 to 681 nm) of the SPR peak with the increase in particle diameter *D* (30-40 nm). This is practically observed for nanocomposites having a higher concentration of Au (see Fig. 10, curves e-g). This effect for larger size particles is called "extrinsic size effect".[5, 25]

The shape and position of the SPR band is also influenced by the dielectric constant of the surrounding environment (here glass) as the resonance condition is $\varepsilon_1 = -2\varepsilon_m$. This constitutes the basis of "immersion spectroscopy".[14] The SPR absorption maxima λ_{max}, is susceptible to the changes of refractive index, n_m of the surrounding medium as:[34, 38, 68]

$$\lambda_{max} = 2\pi c\, m_{eff}\, \varepsilon_o\, [(\varepsilon_\infty + 2n_m^2)]^{1/2} / n_{eff} e^2 \qquad (2)$$

where $n_m = (\varepsilon_m)^{1/2}$, c is the velocity of light and m_{eff} is the effective mass of the electrons. Thus, the SPR peak exhibits a red-shift with increase in medium refractive index.[5, 25] Our antimony glass having a refractive indices in the range 1.9-2.1, radically red-shifts the plasmon peak to around 610 nm. Beside increase in ε_m it is also expected to result an increase in plasmon band intensity and band width.[5, 25] This enables tuning of the SPR peak as shown in Fig. 10. As mentioned earlier, elongated particles may show two maxima if the aspect ratio is ≥ 4.[25, 33, 34, 38] From the TEM images (see Fig. 8c), it is seen that the average aspect ratio of the elliptical Au nanoparticles synthesized within antimony oxide glasses is 1.2. So here only one SPR maxima is displayed.

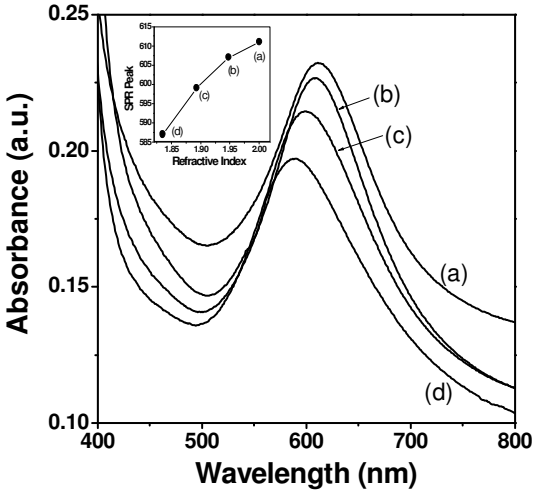

Fig. 10 - SPR band tuning by refractive index control of host glasses. Inset plot shows the red shift of Au^0-SPR band with increase in refractive index of the embedding glass matrix (adapted from Ref. 68).

Nanometal-Bismuth Glass Hybrid Nanocomposites: Synthesis and Effect of Particle Morphology

In recent times, glass researchers have also focused their extensive interest in the bismuth glasses as it is one of the most important among the heavy metal oxide (HMO) glasses due to their several properties[78-81] such as high refractive index, wide transmission window, broad band near infrared (NIR) luminescence, etc. Bismuth glasses have also been found to be very effective for generation of photo induced second harmonic (SHG) as reported by Kityk et al.[82] Bismuth oxide glasses are usually obtained in darkbrown or black color, which deepens with increasing Bi_2O_3 content and when melted at higher temperature.[78, 79, 83] This browning or blackening of bismuth glasses when melted at higher temperature is a serious problem for controlling of Bi^0 NPs and its SPR band which limits their use in optical applications. The intensity of browning or blackening increases with increase in melting temperature as well as Bi_2O_3 concentration due to auto-thermo reduction of Bi^{3+} ions to bismuth metal (Bi^0) during the melting process. The reduction of Bi_2O_3 occurs through the following thermal dissociation reaction[71, 78, 79]

$$2Bi_2O_3 \leftrightarrow 4Bi^0 + 3O_2\uparrow \qquad (3)$$

Hence, it is very difficult to control the nanobismuth particle formation as well as its SPR in bismuth glasses. Therefore, synthesis of controlled Bi^0 NPs[93] in bismuth glasses is very important both academically as well as from technological point of views. Zhang et al.[78] and Sanz et al.[79] have studied the transparency of bismuth glass by addition of color oxidizing additives as dopant such as As_2O_3, Sb_2O_3, CeO_2, etc. However, they have not paid their attention to the above issues.

For first time it was shown by Singh and Karmakar[71] that by the use of suitable oxidizing agents like KNO_3 and $KClO_4$ suitable control of the sizes of spherical Bi nanoparticles, that is, plasmonic properties of Bi nanoparticles in Bi_2O_3 glasses as well as the transparency of the glasses can be controlled. This is shown in Fig. 11. The particle size of the Bi^0 NPs in $KClO_4$ treated glass shows smaller size (2–5 nm) than that of KNO_3 containing glasses (10–15 nm). It is well known that higher the oxidizing power (effectiveness) of the oxidizing agent lower would be the generated Bi^0 particle sizes. Figure 12 shows their TEM, HRTEM and SAED images.

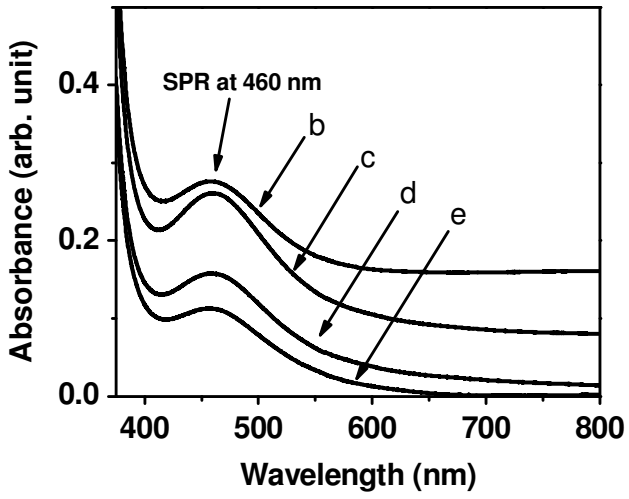

Fig. 11 - Gradual evolution of SPR band of bismuth nanometals in bismuth oxide glasses with increasing oxidizing increasing KNO_3 concentration used as oxidizing agent in their synthesis instead of conventional reducing agent (adapted from Ref. 71)

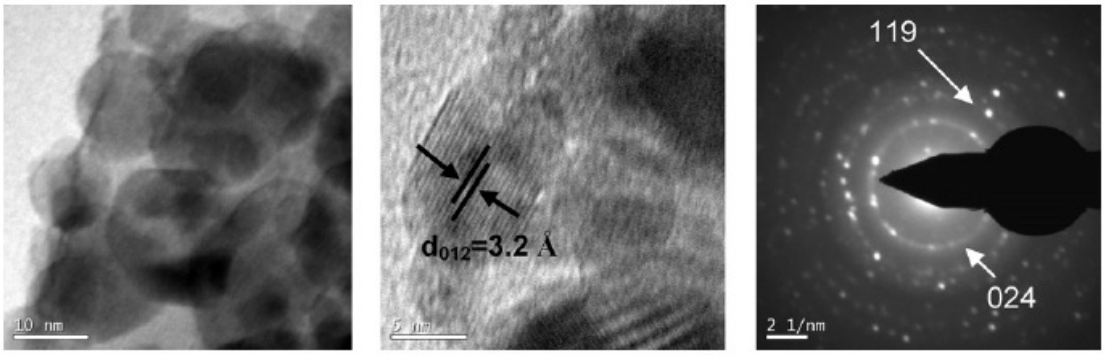

Fig. 12 - TEM image (left), HRTEM (middle) and SAED of bismuth nanometals in bismuth oxide glass nanocomposites (adapted from Ref. 71).

We also synthesized for the first time of hexagonal shaped bismuth coated silver nanoparticles in bismuth glass dichroic (brown in reflection and sky blue in transmission) nanocomposites by a novel and simple one-step melt quench technique.[72] Bismuth glasses on doping with Ag, Ag nanoparticles are first precipitated due to their higher reduction potential followed by precipitation of Bi of it due to their similar lattice constant. At lower concentration of Ag a single SPR maxima is observed (Fig. 13, curve a) due to spherical nanoparticles, but at higher concentration of Ag mixture of spherical and hexagonal nanoparticles are generated (see TEM image Fig. 8i). Formation of hexagonal particles of large aspect ratios is reflected in the UV-vis absorption spectra, which show splitting of the SPR maxima into two peaks (Fig. 13, curve b). The higher energy transverse mode oscillation of the electrons along the minor axis of which absorption maxima is at 575 nm while the lower energy longitudinal mode absorption maxima is at 785 nm corresponding to electron oscillations perpendicular to the major axis. The spectral behavior of the hexagonal nanoparticles is similar to that of a nanorod.[5, 25]

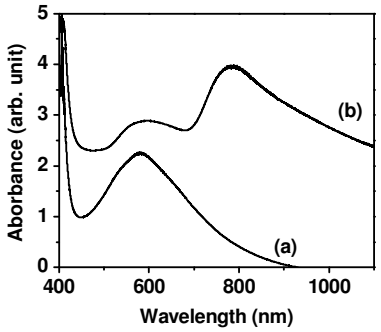

Fig. 13 – Evolution of SPR bands of bismuth coated silver nanoparticles (adapted from Ref. 72).

Nanogold-Tin Phosphate Glass Hybrid Nanocomposites: Effect of Quantum and Dielectric Confinements

According to Eqs. (1) and (2), the SPR maxima are expected to exhibit a red shift with increase in nanoparticle diameter and refractive index respectively. However, a blue-shift is observed in these cases when the particle size remains less than 10 nm. This occurs due to quantum confinement and dielectric confinement effects respectively arising due to the difference in dielectric constant of the confined nanometal and the confining potential barrier around it. We have demonstrated such a blue shift of quantum confined Au nanoparticles in the prototypical tin phosphate glass system.

We fabricated sub-10 nm gold nanoparticles inside tin phosphate glasses by using a new in-situ melt-quench technique without applying any external reducing reagent.[73] UV-visible spectra of these glass nanocomposites show blue shifts (towards lower wavelength) in the SPR band with increase in both nanogold particle size (Fig. 14) and refractive index of the medium (Fig. 15), which are contrary to the common trends according to Eqs. (1) and (2). It is happened due to quantum and dielectric confinements and can be explained by electrodynamics theory.

SPR is due to the contribution of the inter-band electronic term and the Drude term. The SPR involve both conduction electrons and bound electrons. In the visible and ultra-violet region the optical response is dominated by the inter-band term whereas in the red and infrared region the intra-band term (ε_{Drude}) predominates. Polarizations induced by the quasi-unbound and bound electrons bring about the shifting of the SRP band. The plasmon shift is related with both the polarizations induced by the quasi-free and the bound electrons. When the nanoparticle sizes are significantly reduced (quantum confinement), the electronic distribution and polarizability near the surface of the nanoparticle changes due to modification of the electronic wave functions. The plasmonic oscillations (electronic wave functions) extend beyond the nanosphere into the dielectric surroundings over a distance of the order of 0.1 nm since the spherical potential related with the medium is finite.[35] Therefore, the quasi-unbound electrons travel the region which is greater than the diameter D of the nanoparticle and the of electron diameter $D_e > D$.[35] This is called electronic spill-out effect which results in a decrease in the average electron density in the nanoparticle. Hence their contribution to inter-band term is reduced which in turn induces a blue shifting in the SPR bands.[35] They are shown in Figs. 14 and 15. These nanocomposites

embedding quantum dots of gold nanoparticles are also found to be dichroic, transmitting the blue light and reflecting the brown light (see Fig. 8 d-f). This fact is already discussed earlier.

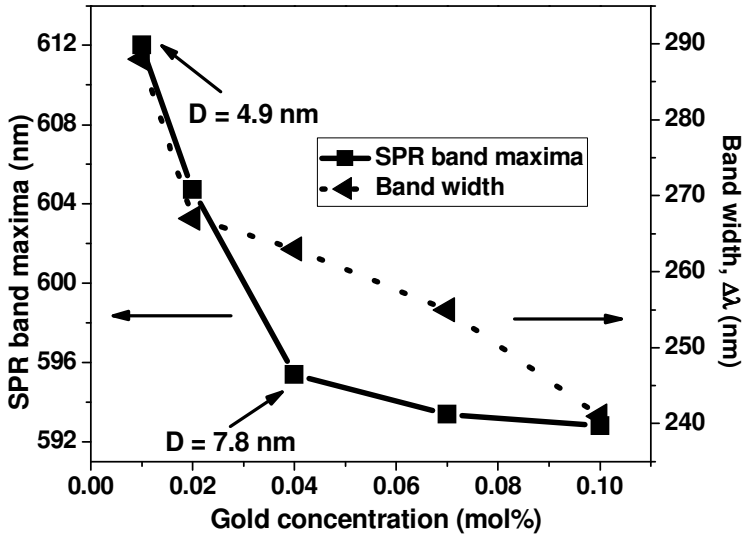

Fig. 14 - Plot of SPR band maxima and width as a function of concentration of gold in nanogold-tin phosphate glass hybrid nanocomposites. Average diameter of gold nanoparticles in two nanocomposites are also shown (adapted from Ref. 73).

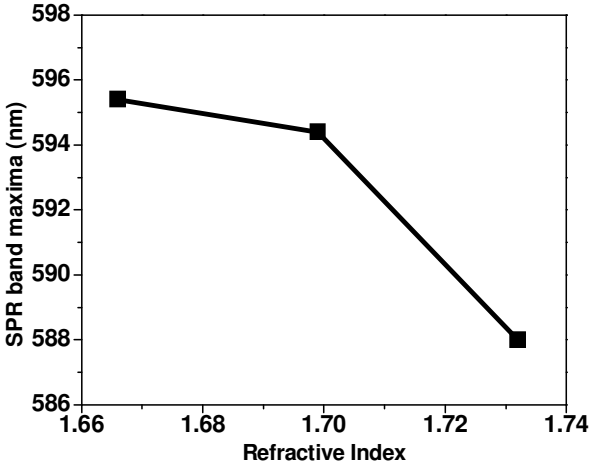

Fig. 15 - Plot of SPR band maxima as a function of refractive index of host glass in nanogold-tin phosphate glass hybrid nanocomposites. (adapted from Ref. 73)

Nanophotonic Application: Nanometal Enhanced Photoluminescence of Rare-Earth Ions

Malta, et al.[84-88] first reported the enhanced photoluminescence (PL) for Eu^{3+} ions in glasses containing silver nanoparticles (NPs). It was also pointed out by them that such enhancements occurred due to the surface plasmon resonance (SPR) of the particles and long range electromagnetic interactions associated with SPR excitation were considered significant in obtaining an enhanced rare-earth (RE) photoluminescence. Hayakawa et al.[89-91] also investigated on Ag–Eu^{3+} co-doped glasses and attributed the observed photoluminescence enhancements to local-field effects owing to the SPR of the metal particles. The plot of electric field amplitude as a function of wavelength of nanogold particles of various sizes[92] is shown in Fig. 16 (a). The SPR absorption band of nanogold as a function of wavelength is also shown in Fig. 16 (b). It is noteworthy that the electric field maxima are at the SPR band peak wavelength. Here it is around 530 nm for gold nanoparticles. It is seen that the electric field amplitude is low at the lower and higher wavelengths of the SPR peak position. These different behaviours are a consequence of a shift in the phase of the nanoparticle polarizability near the SPR band peak wavelength leading to interference effects that vary strongly with wavelength.[92]

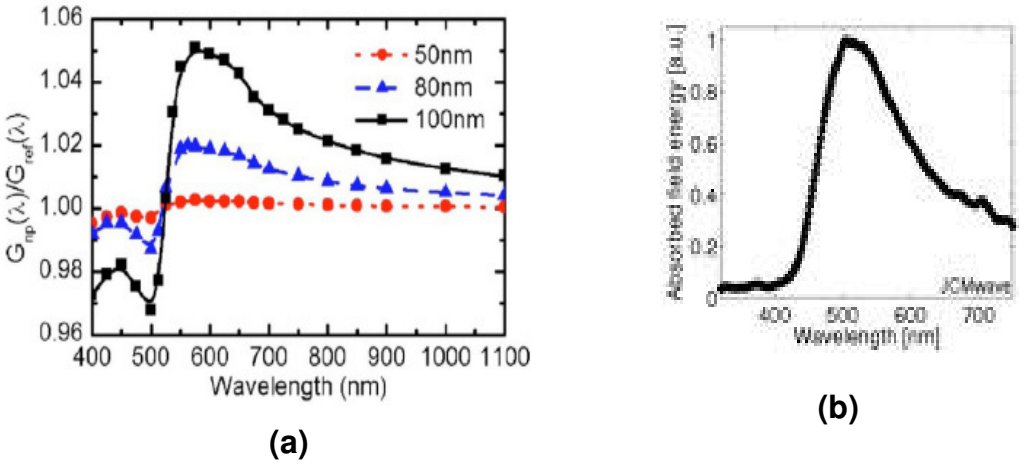

Fig. 17 – (a) Plot of electric field amplitude as a function of wavelength of gold nanoparticles of sizes: 50, 80 and 100 nm. (b) SPR absorption band of nanogold as a function of wavelength (adapted from Ref. 92])

This initiated investigation of metal enhanced fluorescence of RE^{3+} ions in glasses by several groups in the world. Of late, the presence of metallic NPs has also been suggested as accountable for the improved photoluminescence of RE ions in glasses.[93-98] On the other hand, Kassab et al.[99-109] in their investigations of luminescence enhancement of several RE ions in a variety of heavy metal oxide glass matrices (tellurite, lead and bismuth) attributed local field enhancement induced by SPR of metal NPs to be the main cause.

Rare-earth (RE) doped glasses represent an important class of photonic materials owing to their laser amplification and upconversion properties which are critically important to develop short wavelength (visible) lasers, color displays, remote sensing, optical communication, bar-code reading, laser printing, etc.[110-113] However the small absorption cross-section of these RE ions has spawned numerous attempts to enhance the efficiency of these ions. Most concepts rely on energy transfer to the RE^{3+} ions from another species with a large absorption cross-section (Yb^{3+}),[114, 115] energy transfer from another species like SnO_2 nanocrystals,[116] and/or employing low phonon energy host.[110-113] Coupling RE^{3+} ions with metal nanoclusters have recently developed as an interesting alternative strategy to enhance the luminescence intensity of RE^{3+} ions and are likely to bring a renaissance in the field of solid state lasers.[117-120]

The conducting plasmonic metal nanostructures in the vicinity of RE ions are found to alter their free space spectral properties and greatly enhance the yield of their weak optical transitions by precise generation of intense electric fields, i.e., by local field enhancement (LFE) induced by SPR.[10,121] This phenomenon is termed as *'nano metal enhanced fluorescence'* (NMEF). This had initially triggered the numerous basic studies on the effect of metal NPs on the emission properties of RE ions in solution phases and polymers.[122, 123] For example, Wang et al.[122] and Nabika and Deki[123] have reported the enhancement of emissions of Eu^{3+}-complex in solution in presence of Ag. They have mentioned the local field enhancement around the Eu^{3+} ions by the Ag NPs to be the cause of luminescence enhancement.

However, for real application in nanophotonic devices, a major goal has been to produce stable metal nanoclusters within suitable encapsulating hosts. As mentioned earlier, we have witnessed that glasses possess some fantastic properties like high transparency, ease of fabrication in desirable shapes and sizes, inertness, absence of high energy bond vibrations, etc. These have made glasses not only promising encapsulating hosts for lasing RE^{3+} ions but also for

metal NPs. Consequently, nano-metal: rare-earth ions hybrid-glass nanocomposites are currently underway.

Malta et al.[84] and Hayakawa et al.[90] pioneered the nanometal enhanced rare-earth luminescence strudies in silica glasses. Of late, several groups worldwide like Kassab et al.[103] Polman and his co-workers,[124] have initiated this research with heavy metal oxides as glass host. Among the heavy metal oxides, the works so far have mainly been restricted to tellurite, lead and bismuth oxide glasses mainly due to the difficulty of fabrication of antimony glasses. Besides they have mainly employed the traditional techniques to grow spherical nanoparticles within the glasses and the SPR bands. However anisotropic nanoparticles are more potential candidates for luminescence studies because local surface electric fields are drastically increased and confined near the sharp edges of anisotropic nanostructures which act as light-harvesting nanoantennas converting visible light into large localized electromagnetic radiation. This effect is termed as *'lightning-rod effect'*.[121] But the production of anisotropic nanostructures embedded in solid matrices like glasses being a greater challenge, which has been met with a very limited success.

Continuing the process of development, we recently studied the spectroscopic properties of Sm^{3+}, Nd^{3+}, Eu^{3+} and Er^{3+} in a melt-quenched antimony oxide glass system containing nano gold and silver, with the objective of developing a new class of advanced functional nanomaterials and furthering the understanding of optical interactions in these systems.[117-120] We established that the mild reduction capability of Sb_2O_3 enables selective reduction of Au^{3+} ($HAuCl_4.xH_2O$) to Au^0 or Ag^+ ($AgNO_3$ to Ag^0), as the case may be, than RE^{3+} (Sm^{3+}, Er^{3+}, Eu^{3+} and Nd^{3+}) ions (Sm_2O_3, Er_2O_3, Eu_2O_3 and Nd_2O_3) in a single-step during the melting process thereby providing for a straightforward, low-cost strategy for the fabrication of bulk nano metal: RE^{3+} hybrid nanocomposites for application in plasmonics technologies. Besides antimony glasses also have lower phonon energies (602 cm^{-1}) than other heavy metal oxide glasses. This enables efficient upconversion of rare-earth ions reducing the multiphonon relaxation rate. The example of nano-metal enhanced photoluminescence upconversion spectra of Nd^{3+} ions in nanogold-antimony oxide glass nanocomposites is shown Fig. 17. The extent of photoluminescence upconversion intensity enhancement as a function of concentration of gold is also shown in Fig. 18. Maximum amplifications of the 536 nm green and 645 nm red emissions are found to be 8 and 11 fold respectively for nanocomposite containing 0.3 wt.% Nd_2O_3 + 0.03 wt.% Au (Fig. 17, spectrum-c).

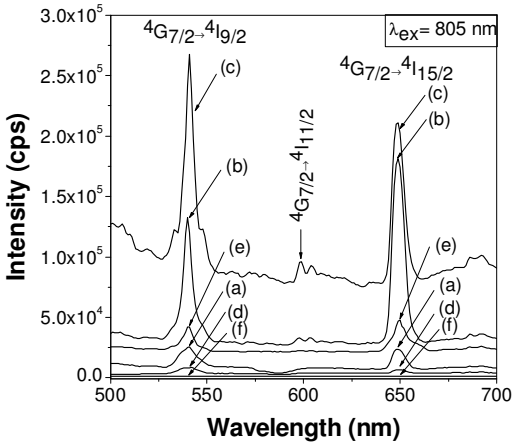

Fig. 17 - Upconversion spectra of glass and nanocomposite containing (a) 0.3 wt.% Nd_2O_3, (b) 0.3 wt.% Nd_2O_3 + 0.003 wt.% Au, (c) 0.3 wt.% Nd_2O_3 + 0.03 wt.% Au, (d) 0.3 wt.% Nd_2O_3 + 0.3 wt.% Au, (e) 0.3 wt.% Au and (f) base glass under excitation wavelength at λ_{ex} = 805 nm The bases of the emission curves a, b, c and e have been uplifted for better visibility (adapted from Ref. 119).

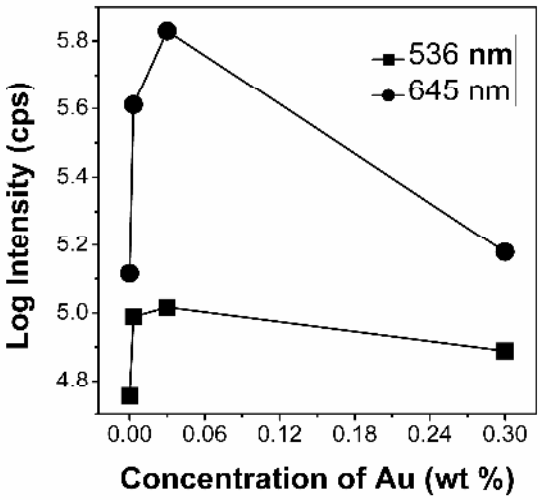

Fig. 18 - Plot of log intensity as a function of concentration of Au (wt %) for 536 and 645 nm emission bands. (adapted from Ref. 119).

Currently there has been a growing controversy regarding the mechanism of enhancement of rare-earth luminescence- whether plasmonic enhancement or energy transfer,[125]

but we believe that the enhanced luminescence is due to local field enhancement (LFE) around the RE^{3+} ions induced by SPR of Au NPs.[90, 103, 110-113] This can be established by electrodynamics theory as described below.

Within the quasistatic approximation, the electric field around a homogeneous and isotropic sphere having radius (a) can be written as:[1-11]

$$E_{out} = |E_0|\hat{x} - \alpha|E_0| \left[\frac{\hat{x}}{r^3} - \frac{3x\,(\hat{x}x + \hat{y}y + \hat{z}z)}{r^5} \right] \quad (4)$$

x, y, and z are the Cartesian coordinates, *r* is the radial distance, and $\hat{x}$, $\hat{y}$, and $\hat{z}$ are the unit vectors. $\boldsymbol{E}_0$ is the incident electromagnetic field vector pointing along the *x*-axis and independent of coordinates for distances on the order of the dimension of the sphere. The first term here is the applied field of the light and the second is the induced dipole of the polarized sphere. α is the static metal polarizability and is given as:[1-11]

$$\alpha = 4\pi a^3 \frac{\varepsilon_{Au} - \varepsilon_m}{\varepsilon_{Au} + 2\varepsilon_m} \quad (5)$$

The polarizability and thus the induced homogeneous polarization inside the particle are resonantly enhanced at the plasmon frequency where the denominator shows a minimum, that is, the real part of the dielectric constant of the metal (here considering Au) ε_{Au} that is, $\varepsilon_1 = -2\varepsilon_m$ and the imaginary part (ε_i) is small, α becomes large producing an improved induced field. Thus SPR is an essential condition for effective enhancement processes. It is also interesting to note that the plasmon resonance is not only determined by ε_{Au}, but also by ε_m. At the plasmon resonance, the near field of the nanoparticles is disturbed. Thus such enhancements of the electromagnetic field at the interface are responsible for surface-enhanced optical phenomena. When the RE^{3+} ions are present within close ranges of such conducting metallic NPs, experience a drastic increase in their excitation rates by the induced enhanced near-electric field intensities (i.e. by local field enhancement).

All of the above categories of metal-glass nanocomposites make them potential for applications in the optical memory devices with high storage density and ultrafast recording speed, various other nanophotonic and optoelectronic devices.

Plasmon-Based Nanophotonic Applications

"Nanophotonics" is another emerging multidisciplinary field that enables exploitation of study light–matter interactions on a scale much smaller than the wavelength of light.[5] The applications of nanophotonics are ample. Several nanophotonic applications thrive on the exploitation of plasmonics which currently is seriously being considered as a promising approach to tackle important global issues such as energy generation and even healthcare.[1-12, 124]

When surface plasmons are localized in or around metal nanostructures, a wealth of interesting optical effects arises, such as local electric field enhancement near the interface of the nanometal and dielectric.[5,25] This local field enhancement has fostered great expectations in new applications of plasmonic structures.[5,6] Some of the most prevalent application of nanostructured materials which utilizes the evanescent field at the surface are surface enhanced fluorescence, surface enhanced Raman scattering (SERS), surface plasmon resonance imaging and spectroscopy, optical/ molecular sensors, surface enhanced second harmonic generation, photothermal imaging and therapy, photonic circuitry, optical communications and non-linear optical elements.[1-12, 25] The major advantage of plasmon-based nanostructures is that light can be confined to and manipulated on a scale smaller than the wavelength of light (a few hundred nanometers), i.e., smaller than would be possible by conventional optics.[32, 92] Metal nanoparticle arrays supported by suitable matrices (optical glasses, fibers or polymers) can serve to transport /guide electromagnetic energy in the visible and infrared wavelengths over distances of tens to hundreds of micrometers.[32] Very tight lateral confinement of light can be achieved by use of linear arrays of metal nanoparticles.[8-10] Surface plasmon based photonic devices not only offer the opportunity to develop high quality optical communication systems by integrating photonic and electronic circuits but can also result in intense light generation from luminescent materials.[11-17]

Conclusions

In this review, with a short historical background, preparation of a variety of nanometal-glass hybrid nanocomposites by different multi-step techniques, properties and applications are briefly described. In addition, recently developed single-step in-situ thermochemical reduction methodology by these authors for their synthesis is described in details with their characteristic properties, relevant theories and applications. Here Au, Ag, and Bi metals are considered and the glasses addressed are based on antimony, bismuth and phosphorus oxides. Some of them are dichroic in nature, that is, they exhibit blue to green colorations in transmitted light and brown to reddish brown colorations in reflected light. Both spherical and non-spherical gold or silver nanoparticles could exhibit dichroism. The appropriate reasons for their dichroic character are still remained unsettled. The solution leftovers open for the researchers. Nanometal-antimony oxide glass nanocomposites have been found to enhance the photoluminescence upconversion intensities up to 11 fold when co-doped with rare-earth oxides (for example, Nd_2O_3, Er_2O_3, and Sm_2O_3) due to the plasmonic induced local field enhancement effects of metal nanoparticles. These studies have revealed that nanometal-glass hybrid nanocomposites are very promising for various nanophotonic applications, such as nanometal enhanced rare-earth luminescence, solar cell, light emitting diode, plasmonic integrated circuit, plasmon slot waveguide, etc. The reasons for the present excitement in the nanometal-glass hybrid nanocomposites research are because of their several inherent advantages over other dielectric nanocomposites, exceptional properties, unique functions in nanoscience and future nanotechnology.

Acknowledgements: The authors are thankful to Prof. Indranil Manna, Director, CGCRI for his kind permission to publish this paper. TS gratefully thanks CSIR, New Delhi for the financial support in the form of NET-SRF Research Fellowship. The financial support of the NMITLI Scheme of CSIR is thankfully acknowledged. SPS would also like to thank CSIR for the award of Senior Research Fellowship (SRF).

References

1. A. M. Schwartzberg and J. Z. Zhang, *J. Phys. Chem.,* **C112**, 10323-10337 (2008).

2. X. Lu, M. Rycenga, S. E. Skrabalak, B. Wiley and Y. Xia, *Ann. Rev. Phys. Chem,*. **60**, 167192 (2009).

3. M. Bäumer and H. –J. Freund, *Prog. Surf. Sci.,* **61**, 127-139 (1999).

4. E. Ozbay, *Science,* 311, 189-193 (2006).

5. P. N. Prasad, *Nanophotonics,* pp. 129-151, Wiley, New Jersey, 2004.

6. W. A. Murray and W. L. Barnes, *Adv. Mater.,* **19**, 3771–3782 (2007).

7. S. A. Maier and H. A. Atwater, *J. Appl. Phys.* **98**, 011101 (10 pp.) (2005).

8. W. L. Barnes, A. Dereux and T. W. Ebbesen, *Nature,* **424,** 824-830 (2003).

9. F. Le, D. W. Brandl, Y. A. Urzhumov, H. Wang, J. Kundu, N. J. Halas, J. Aizpurua and P. Nordlander, *ACS Nano,* **2,** 707-718 (2008).

10. S. Lal, S. Link and N. J. Halas, *Nature Photonics,* **1**, 641-648 (2007).

11. C. D. Geddes and J. R. Lakowicz, *J. Fluoresc.* **12**, 121-129 (2002).

12. K. Aslan, I. Gryczynski, J. Malicka, E. Matveeva, J. R Lakowicz and C. D Geddes, *Current Opinion Biotechnol.* **16**, 55–62 (2005).

13. J. R. Lakowicz, K. Ray, M. Chowdhury, H. Szmacinski, Y. Fu, J. Zhang and K. Nowaczyk, *Analyst,* **133**, 1308–1346 (2008).

14. C. D. Geddes, I. Gryczynski, J. Malicka, Z. Gryczynski and J. R. Lakowicz, *Combinat. Chem. High Throughput Screening,* **6**, 109-117 (2003).

15. J. R. Lakowicz, B. P. Maliwal, J. Malicka, Z. Gryczynski and I. Gryczynski, *J. Fluoresc.* **12**, 431-437 (2002).

16. E. G. Matveeva, I. Gryczynski, A. Barnett, Z. Leonenko, J. R. Lakowicz and Z. Gryczynski, *Anal. Biochem.* **363**, 239-245 (2007).

17. A. V. Zayats, I. I. Smolyaniov and A. A. Maradudin, *Phys. Reports,* **408**, 131-314 (2005).

18. F. E. Wagner, S. Haslbeck, L. Stievano, S. Calogero, Q. A. Pankhurst and K.-P. Martinek, *Nature,* **407**, 691-692 (2000).

19. L. M. Liz-Marzán, *Mater. Today,* **7**, 26-31 (2004).

20. Freestone, N. Meeks, M. Sax and C. Higgitt, *Gold Bull.,* **40**, 270-277 (2007).

21. J. Kunckel, *Ars Vitraria Experimentalis oder vollkommene Glasmacher-Kunst*, Berlegung Christoph Riegels, Frankfurt,1689.

22. W. A. Weyl, *Coloured Glasses*, Society of Glass Technology, Sheffield, 1951.

23. M. Valden, X. Lai and D. W. Goodman, *Science,* **281**, 1647–1650 (1998).

24. P. Buffat and J. P. Borel, *Phys. Rev. A,* **13,** 2287–2298 (1976).

25. U. Kreibig, and M. Vollmer, *Optical Properties of Metal Cluster,* Springer: Berlin, 1995.

26. E. Hutter and J. H. Fendler, *Adv. Mater.,* **16,** 1685-1706 (2004).

27. F. Gonella and P. Mazzoldi,"*Metal Nanocluster Composite Glasses*" In: *Handbook of Nanostructured Materials and Nanotechnology*, H. S. Nalwa (editor), vol 4, Academic Press, San Diego, 2000.

28. K. L. Kelly, E. Coronado, L. L. Zhao and G. C. Schatz, *J. Phys. Chem. B,* **107,** 668-677 (2003).

29. G. C. Papavassiliou, *Prog. Solid State Chem.,* **12,** 185-271 (1979).

30. C. F. Bohren and D. R. Huffman, *Absorption and Scattering of Light by Small Particles,* Wiley: New York, 1983.

31. S. K. Ghosh and T. Pal, *Chem. Rev.,* **107,** 4797-4862 (2007).

32. W. L. Barnes, A. Dereux, and T. W. Ebbesen, *Nature,* **424**, 824-830 (2003).

33. P. Mulvaney, *Langmuir,* **12,** 788-800 (1996).

34. C. Noguez, *J. Phys. Chem. C,* **111**, 3806-3819 (2007).

35. F. Vallée, in; *Nanomaterials and Nanochemistry*, C. Bréchignac, P. Houdy and M. Lahmani (Eds.), Springer-Verlag, Berlin Heidelberg, 2007.

36. C. Bréchignac, Ph. Cahuzac, J. Leygnier and A. Sarfati, *Phys. Rev. Lett.*, **70**, 2036-2039 (1993).

37. C. Voisin, D. Christofilos, N. Del Fatti and F. Vallée, *Phys. Rev. Lett.,* **85,** 2200-2204 (2000).

38. S. Link and M. A. El-Sayed, *Internat. Rev. Phys. Chem.,* **19**, 409-453 (2000).

39. J. Pérez-Juste, I. Pastoriza-Santos, L. M. Liz-Marzán and P. Mulvaney, *Coordinat. Chem. Rev*. 249 1870–1901 (2005).

40. G. Schmid, *"General Features of Metal Nanoparticles Physics and Chemistry"* In: *Metal Nanoclusters in Catalysis and Materials Sscience: The Issue of Size Control* B. Corain, G. Schmid, and N. Toshima (eds), Elsevier, Amsterdam, 2008, pp. 3-20.

41. D. D. Evanoff, Jr. and G. Chumanov, *Chem. Phys. Chem.,* **6**, 1221–1231 (2005).
.
42. S. Inasawa, M. Sugiyama and Y. Yamaguchi, *J. Phys. Chem. B,* **19,** 9404-9410 (2005).

43. E. A. Coronado and G. C. Schatz, *J. Phys. Chem.,* **119**, 3926-3934 (2003).

44. Y. Hamanaka, K. Fukata, A. Nakamura, L. M. Liz-Marzán and P. Mulvaney, *Appl. Phys. Lett.,* **84**, 4938 (3 pp.) (2004).

45. L. M. Liz-Marzán, *Langmuir,* **22,** 32-39 (2006).

46. M. C. Daniel and D. Astruc, *Chem. Rev.,* **104,** 293-346 (2004).

47. V. Myroshnychenko, J. Rodríguez-Fernández, I. Pastoriza-Santos, A. M. Funston, C. Novo, P. Mulvaney, L. M. Liz-Marzán and F. J. G. de Abajo, *Chem. Soc. Rev.,* **37**, 1792–1805 (2008).

48. S. Chen, T. Akai, K. Kadono and T. Yazawa, *Appl. Phys. Lett.,* **79**, 3687 (3 pp.) (2001).

49. H. Zeng, J. Qiu, S. Yuan, Y. Yang, G. Chen, *Ceram. Internat.,* **34**, 605–608 (2008).

50. H. Zeng, J. Qiu, X. Jiang, C. Zhu and F. Gan, *J. Cryst. Growth,* **262**, 255–258 (2004).

51. H. Zeng, G. Chen, J. Qiu, X. Jiang, C. Zhu and F. Gan, *J. Non-Cryst. Solids,* **354**, 1155–1158 (2008).

52. M. V. Roldán, A. Frattini, O. de Sanctis, H. Troiani and N. Pellegri, *Appl. Surf. Sci.,* **254**, 281–285 (2007).

53. S. Chen, T. Akai, K. Kadono and T. Yazawa, *Chem. Commun.* **20**, 2090–2091 (2001).

54. R. H. Doremus, *J. Chem. Phys.,* **40**, 2389-2396 (1964).

55. R. H. Doremus, *J. Appl. Phys.,* **35**, 3456-3463 (1964).

56. J. Shin, K. Jang, K. –S. Lim, I. –B. Sohn, Y. –C. Noh and J. Lee, *Appl. Phys, A,* **93,** 923–927 (2008).

57. G. Speranza, L. Minati, A. Chiasera, M. Ferrari, G. C. Righini and G. Ischia, *J. Phys. Chem. C,* **113**, 4445-4450 (2009).

58. H. Hofmeister, W. –G. Drost and A. Berger, *Nanostruct. Mater.,* **12**, 207-210 (1999).

59. M. Kaempfe, T. Rainer, K. -J. Berg, G. Seifert and H. Graener, *Appl. Phys. Lett.,* **74**, 1200-1202 (1999).

60. D. P. Peters, C. Strohhöfer, M.L. Brongersma, J. van der Elsken, and A. Polman, *Nucl. Inst. Methods Phys. Res. B,* **168**, 237-244 (2000).

61. M. Dubiel, H. Hofmeister and E. Wendler, *J. Non-Cryst. Solids,* **354**, 607–611 (2008).

62. P. Gangopadhyay, P. Magudapathy, R. Kesavamoorthy, B.K. Panigrahi, K.G.M. Nair and P.V. Satyam, *Chem. Phys. Lett.,* **388**, 416–421 (2004).

63. H. Zeng, C. Zhao, J. Qiu, Y. Yang and G. Chen, *J. Cryst. Growth,* **300**, 519–522 (2007).

64. Kassab L. R. P. Kassab, D. S. de Silva, R. de Almeida and C. B. de Araújo, *Appl. Phys. Lett.,* **94**, 101912 (3pp.) (2009).

65. S. Qu, C. Zhao, X. Jiang, G. Fang, Y. Gao, H. Zeng, Y. Song, J. Qiu, C. Zhu and K. Hirao, *Chem. Phys. Lett.,* **368**, 352-355 (2003).

66. H. D. Schreiber, M. A. Stone and A. M. Swink, *J. Non-Cryst. Solids,* **352**, 534-538 (2006).

67. T. Som and B. Karmakar, *Appl. Surf. Sci.,* **255**, 9447–9452 (2009).

68. T. Som and B. Karmakar, *Chem.Phys. Lett.,* **479**, 100–104 (2009).

69. T. Som and B. Karmakar, *Plasmonics,* (2010) (In Press).

70. T. Som and B. Karmakar, *Nano Research,* **2**, 607-616 (2009).

71. S. P. Singh and B. Karmakar, *Mater. Chem. Phys.,* **119**, 355–358 (2010).

72. S. P. Singh and B. Karmakar, *Chem. Mater.,* (2010) (Communicated).

73. M. Nath, S. P. Singh and B. Karmakar, *Nanostruct. Res. Lett.,* (2010) (Communicated).

74. http://en.wikipedia.org/wiki/Transmission_electron_microscopy

75. M. Kaempfe, G. Seifert, K. –J. Berg, H. Hofmeister and H. Graener, *Eur. Phys. J. D.,* **16,** 237-240 (2001).

76. E. Fort, C. Ricolleau and J. Sau-Pueyo, *Nano Lett.,* **3**, 65-67 (2003).

77. G. Mie, *Ann. Physik (Leipzig),* **25,** 377-445 (1908).

78. Y. Zhang, Y. Yang, J. Zheng, W. Hua and G. Chen, *J. Am. Ceram. Soc.,* **91**, 3410-3417 (2008).

79. O. Sanz, E. Haro-Poniatowski, J. Gonzalo and J.M. Fernández Navarro, *J. Non-Cryst. Solids, **352**, 761-769 (2006).*

80. S. Khonthon, S. Morimoto, Y. Arai and Y. Ohishi, *Opt. Mater.,* **31**, 1262-1271 (2009).

81. S. Zhou, N. Jiang, B. Zhu, H. Yang, S. Ye, G. Laksminarayana, J. Hao and J. Qiu, *Adv. Funct. Mater.,* **18**, 1407-1411 (2008).

82. I.V. Kityk, W. Imiolek, A. Majchrowski and E. Michalski, *Opt. Commun.,* **219**, 421-427 (2003).

83. W. Li, *Mater. Chem. Phys.,* **99**, 174-179 (2006).

84. O. L. Malta, P. A. Santa-Cruz, G. F. De Sá and F. Auzel, *J. Lumin.,* **33**, 261-272 (1985).

85. G. F. de Sá, W. M. de Azevedo, O. L. O. L. Malta, P. A. Santa-Cruz, G. F. De Sá and F. Auzel, *Chem. Phys. Lett.,* **116**, 396-399 (1985).

86. O. L.Malta, *J. Lumin.,* **40-41**, 133-134 (1988).

87. O.L. Malta, P.A. Santa-Cruz, G.F. de Sa´ and F. Auzel, *J. Solid State Chem.,* **68**, 314-319 (1987).

88. G. F. De Sá, O. L. Malta, W. M. De Azevêdo and H. Dexpert, *J. Less Common Metals,* **148**, 387-391 (1989).

89. T. Hayakawa, S. T. Selvan and M. Nogami, *J. Non-Cryst. Solids,* **259**, 16-22 (1999).

90. T. Hayakawa, S. T. Selvan and M. Nogami, *Appl. Phys. Lett.,* **74,** 1513 (3 pp.) (1999).

91. T. Hayakawa, S. T. Selvan and M. Nogami, *J. Phys. Chem. B,* **103**, 7064-7067 (1999).

92. S. H. Lim, W. Mar, P. Mathieu, D. Derkacs and E. T. Yu, J. Appl. Phys., **101**, 104309 (7 pp.) (2007).

93. M. Fukushima, N. Managaki, M. Fujii, H. Yanagi and S. Hayashi, *J. Appl. Phys.,* **98**, 24316 (4 pp.) (2005).

94. T. Aisaka, M. Fujii and S. Hayashi, *Appl. Phys. Lett.,* **92**, 132105 (3 pp.) (2008).

95. J. C. Pivin, M. Sendova-Vassileva, G. Lagarde, F. Singh and A. Podhorodecki, *J. Phys. D: Appl. Phys.,* **39**, 2955-2958 (2006).

96. J. Ueda, S. Tanabe and A. Ishida, *J. Non-Cryst. Solids.,* **355**, 1912–1915 (2009).

97. J. Ebothe, K. Ozga, A. Ali Umar, M. Oyama and I.V. Kityk, *Appl. Surf. Sci.,* **253**, 1626–1630 (2006).

98. P. R. Watekar, S. Ju and W. T. Han, *Colloids and Surfaces A: Physicochem. Engg. Aspects,* **313-314**, 492-496 (2008).

99. A. P. Carmo, M. J. V. Bell, V. Anjos, R. de Almeida, D. M. da Silva and L. R. P. Kassab, *J. Phys. D: Appl. Phys.,* **42**, 155404 (5 pp.) (2009).

100. R. de Almeida, D. M. da Silva, L. R.P. Kassab and C. B. de Araújo, *Opt. Commun.,* **281**, 108–112 (2008).

101. L. R. P. Kassab, R. de Almeida, D. M. da Silva, T. A. A. de Assumpção and C. B. de Araújo, *J. Appl. Phys.,* **105,** 103505 (6 pp.) (2009).

102. T. A. A. de Assumpção, D. M. da Silva, L. R. P. Kassab and C. B. de Araújo, *J. Appl. Phys.,* **106**, 0635222 (7 pp.) (2009).

103. L. R. P. Kassab, D. S. da Silva, R. de Almeida and C. B. de Araújo, *Appl. Phys. Lett.,* **94**, 101912 (3 pp.) (2009).

104. L. R. P. Kassab, R. de Almeida, D. M. da Silva, and C. B. de Araújo, *J. Appl. Phys.,* **104**, 093531 (5 pp.) (2008).

105. V. K. Rai, L. de S. Menezes, C. B. de Araújo, L. R. P. Kassab, D. M. da Silva and R. A. Kobayashi, *J. Appl. Phys.,* **103**, 093526 (6 pp.) (2008).

106. L. R. P. Kassab, C. B. de Araújo, R. A. Kobayashi, R. de Almeida Pinto and D. M. da Silva, *J. Appl. Phys.,* **102**, 103515 (7 pp.) (2007).

107. L. P. Naranjo, C. B. de Araújo, O. L. Malta, P. A. Santa Cruz, and L. R. P. Kassab, *Appl. Phys. Lett.* **87**, 241914 (3 pp.) (2005).

108. C. B. de Araújo, L. R. P. Kassab, R. A. Kobayashi, L. P. Naranjo and P. A. Santa Cruz, *J. Appl. Phys.,* **99**, 123522 (7 pp.) (2006).

109. L. R. P. Kassab, F. A. Bomfim, J. R. Martinelli, N. U. Wetter, J. J. Neto and C. B. de Araújo, *Appl. Phys. B: Lasers and Optics,* **94**, 239-242 (2008).

110. T. Som and B. Karmakar, *J. Phys.: Cond. Matter,* **22**, 035603 (11 pages) (2010).

111. T. Som and B. Karmakar, *Opt. Mater.,* 31, 609–618 (2009).

112. T. Som and B. Karmakar, *J. Alloys Comp.,* **476**, 383–389 (2009).

113. T. Som and B. Karmakar, *J. Lumin.,* **128**, 1989–1996 (2008).

114. X. Wang, *Spectrochim. Acta A: Molecular & Biomolecular Spectros.,* **70**, 99-103 (2008).

115. L. Lu, Q. Nie, X. Shen, S. Dai, T. Xu, Z. Jin, Y. Shen and X. Zhang, *Spectrochim. Acta A: Molecular & Biomolecular Spectros.,* **67,** 1228-1231(2007).

116. T. Hayakawa and M. Nogami, *Sci. Technol. Adv. Mater.,* **6,** 66-70 (2005).

117. T. Som and B. Karmakar, *J. Appl. Phys.,* **105**, 013102 (8 pp) (2009).

118. T. Som and B. Karmakar, *J. Opt. Soc. Am. B,* **26**, B21-B27 (2009).

119. T. Som and B. Karmakar, *Solid State Sci.,* **11,** 1044–1051 (2009).

120. T. Som and B. Karmakar, *Spectrochim. Acta A: Molecular & Biomolecular Spectros.,* **75**, 640–646 (2010).

121. C. D. Geddes and J. R. Lakowicz, *J. Fluoresc.,* **12**, 121-129 (2002).

122. Y. Wang, J. Zhou and T. Wang, *Mater. Lett.,* **62**, 1937–1940 (2008).

123. H. Nabika and S. Deki, *J. Phys. Chem. B,* **107**, 9161-9164 (2003)

124. J. Kalkman, L. Kuipers, A. Polman and H. Gersen, *Appl. Phys. Lett.,* **86**, 041113 (3 pp.) (2005).

125. M. Eichelbaum and K. Rademann, *Adv. Funct. Mater.,* **19,** 1–8 (2009).